JOURNAL OF MATERIALS SCIENCE 13 (1978) 580–586

Determination of tensile and compressive creep behaviour of ceramic materials from bend tests*

PATRICK K. TALTY
Chemistry and Materials Science Department, Lawrence Livermore Laboratory, University of California, Livermore, California 94550, USA

RICHARD A. DIRKS
Air Force Flight Dynamics Laboratory, Air Force Wright Aeronautical Laboratories (AFSC), Wright-Patterson AFB, Ohio 45433, USA

We have developed equations that permit the determination of individual compressive and tensile creep rates from four-point bend test measurements made on trapezoidal bars. The equations developed are for the general stress dependence case. Finnie first proposed this type of analysis and solved the equations for the case of linear stress dependence. We present graphs that show solutions to the equations for the stress squared case. Creep measurements were performed on trapezoidal HS-130 Si_3N_4 bars to determine the ratio of compressive to tensile creep (β). The values determined on four separate tests using two different temperatures and beam dimension ratios b_2/b_1 gave fairly consistent results. The β's for previously unstrained material are: 0.24, 0.14, 0.17, and 0.17 with the average value of $\beta = 0.18$. For the case of prestrained Si_3N_4, β is 0.48. To further test the usefulness of this analysis, data from a conventional (rectangular bars) four-point bend test were taken from the literature and analysed using the equations developed in this paper and the average determined value of β. The individual tensile and compressive creep rates determined in this manner were found to agree very closely with other literature data measured in direct tension and compression tests.

1. Introduction

The four-point bend test is often used to obtain information about the high-temperature tensile creep behaviour of ceramic materials. This test is easy to perform and avoids the problems of alignment and fixturing commonly associated with uniaxial tensile testing of brittle materials [1, 2]. In analysing bend test data it is usually assumed that the neutral axis passes through the centroid of cross-sectional area of the test piece [2, 3]. For this assumption to be valid, the creep behaviour of the material must be the same in both tension and compression. However, recent work [4–6] on hot-pressed silicon nitride (Si_3N_4), a candidate material for high performance turbine applications, has shown that there is a large difference between the tensile and compressive creep behaviour of this material. Using an idealized model, Lange [7] showed that, in general, polycrystalline materials with a viscous boundary phase (such as hot-pressed Si_3N_4) will exhibit a much greater rate of deformation in tension than in compression.

The purpose of this paper is to present an experimental technique for using four-point bend tests on trapezoidal beams to determine the individual tensile and compressive creep rates of a material.

*The experimental work was performed at the Metallurgy and Ceramics Laboratory, Aerospace Research Laboratories (AFSC), Wright-Patterson AFB, Ohio, USA.

Finnie [8] originally proposed the technique and solved the governing equations for the case of a linear dependence of creep rate on stress. This paper extends the analysis to an arbitrary stress dependence, and then presents solutions for the specific case where the creep rate depends on the square of the stress. The technique was used to analyse four-point bending tests on HS-130 hot-pressed Si_3N_4 from Norton Co.* in order to determine its tensile and compressive creep behaviour. These results are compared with data available in the literature.

2. Analysis and development of equations

In this section, we develop the equations that relate material response and specimen geometry to experimental data. Parameters of interest are:

β, the ratio of compressive to tensile creep strain.

n, the stress exponent in the general creep law.

b_1 and b_2, known specimen dimensions.

δ and δ', measured four-point bending centre-point deflections obtained under identical conditions of bending moment, M, and temperature for geometries of Figs. 1a and b, respectively. Our analysis characterizes the specimen width, b, and stress, σ, as functions of distance, y, from the (as yet undetermined) neutral axis location. In general, both n and β may be unknown. One approach is to assume a value for n and proceed as detailed in Section 4. A second approach is to use the equations of force and moment equilibrium to form a set of nonlinear equations and seek solutions numerically.

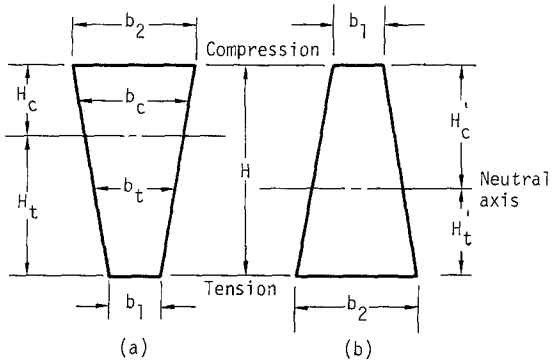

Figure 1 Nomenclature and orientation of trapezoidal cross-section beams. H_c is the distance from the neutral axis of the beam to the outer compressive fibre and H_t is the distance to the outer tensile fibre.

The first approach is used in this paper.

The material is assumed to respond according to a creep law of the form

$$\epsilon = A\sigma^n F(t), \tag{1}$$

where $F(t)$ is an arbitrary function of time common to both tensile and compressive creep, and A is a constant, which may vary between tensile and compressive creep, but is constant with respect to time. The constitutive law of creep compliance for a material is usually assumed [2] to be of this form. The creep rate is then given by the time derivative of Equation 1,

$$\dot{\epsilon} = A\sigma^n F'(t). \tag{1A}$$

The strain time response of most materials under creep conditions shows a constant or steady-state creep rate over most of their total strain compliance [9], where $F'(t) = K$ (constant). The ratio of A (compressive creep) to A' (tensile creep) at a given stress is defined as β. The assumption that the tensile and compressive creep strain show the same time dependence, i.e. $K_{(\text{compressive})} = K_{(\text{tensile})}$, appears reasonable, but in any case this analysis allows this assumption to be verified.

Plane sections through a beam are assumed to remain plane, so that;

$$\epsilon(y) = \epsilon_{\max}\left(\frac{y}{y_{\max}}\right), \tag{2}$$

where y is the distance from the neutral axis. The slope of the beam will be assumed to be sufficiently small so that the approximation†

$$\frac{1}{R} = \frac{d^2Y}{dx^2}\left[1 + \left(\frac{dY}{dx}\right)^2\right]^{3/2} \simeq \frac{d^2Y}{dx^2}$$
$$\left.\frac{d^2Y}{dx^2}\right|_{\text{centre point}} \simeq \frac{8\delta}{l^2} \tag{3}$$

may be made, where R is the radius of curvature, x is the distance along the length of the beam between the inner load points, l is the distance between the inner load points, and Y and δ are vertical deflections; Y is a function of position along the beam, and y is the deflection at the centre of the beam.

*Reference to a company or product name does not imply approval or recommendation of the product by the University of California or the US Energy Research and Development Administration to the exclusion of others that may be suitable.

†This assumption introduces less than 0.2% error in the analysis of the creep data in this paper.

Care must be exercised to avoid complex numbers in the development of the following equations. This difficulty is accomplished by evaluating the integrals piecewise, over positive domains of y. Accordingly, the following two equations describe the specimen width, b, as functions of distance from the neutral axis (Fig. 1);

$$b_c(y) = b_2 - \left(\frac{b_2 - b_1}{H}\right)(H_c - y), 0 \leqslant y \leqslant H_c$$

$$b_t(y) = b_1 + \left(\frac{b_2 - b_1}{H}\right)(H_t - y), 0 \leqslant y \leqslant H_t. \tag{4}$$

In a manner directly analogous to that detailed by Finnie [8], stresses for the general case are given by;

$$\sigma_c(y) = \sigma_{H_c}\left(\frac{y}{H_c}\right)^{1/n}, 0 \leqslant y \leqslant H_c$$

$$\sigma_t(y) = \sigma_{H_c}\left(\frac{\beta y}{H_c}\right)^{1/n}, 0 \leqslant y \leqslant H_t, \tag{5}$$

and the force equilibrium equation for bending, expressed piecewise, becomes

$$\int_{-H_t}^{H_c} \sigma(y)\mathrm{d}A = \int_0^{H_c} \sigma_c(y)b_c(y)\mathrm{d}y - \int_0^{H_t} \sigma_t(y)b_t(y)\mathrm{d}y = 0, \tag{6}$$

which after normalizing with respect to beam height ($h_c = H_c/H$, $h_t = H_t/H$) and collecting terms becomes, for the geometry of Fig. 1a,

$$\beta^{1/n}(1-h_c)^{1+1/n}\left[1 + \left(\frac{n}{2n+1}\right)\left(\frac{b_2}{b_1} - 1\right)(1-h_c)\right] - h_c^{1+1/n}\left[\frac{b_2}{b_1} - \left(\frac{n}{2n+1}\right)\left(\frac{b_2}{b_1} - 1\right)h_c\right] = 0 \tag{7}$$

Due to symmetry, the equation for the complementary geometry of Fig. 1b may be obtained by substituting $\frac{1}{\beta}$ and h_t' for β and h_c, respectively. Solutions of Equation 7 for the case of $n = 2$ are presented graphically for a range of $\frac{b_2}{b_1}$ and β in Fig. 2.

Taking

$$C = \frac{(2n+1)M}{nb_1H^2},$$

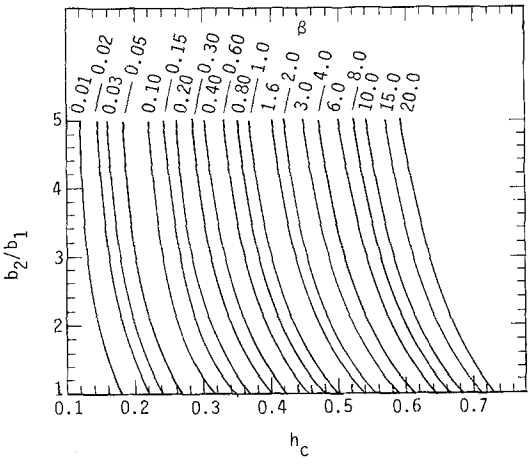

Figure 2 Graphical solutions of Equation 7 for $n = 2$. This graph is used to locate the depth of the neutral axis h_c versus b_2/b_1 for a series of β's.

the equation of moment equilibrium

$$\int_{-H_t}^{H_c} \sigma(y)y\mathrm{d}A = \int_0^{H_c} \sigma_c(y)b_c(y)y\mathrm{d}y - \int_0^{H_t} \sigma_t(y)b_t(y)y\mathrm{d}y = M \tag{8}$$

becomes, for the geometry of Fig. 1a,

$$\frac{Ch_c^{1/n}}{\sigma H_c} = h_c^{2+1/n}\left[\frac{b_2}{b_1} - \left(\frac{n}{3n+1}\right)\left(\frac{b_2}{b_1} - 1\right)h_c\right] + \beta^{1/n}(1-h_c)^{2+1/n}\left[1 + \left(\frac{n}{3n+1}\right)\left(\frac{b_2}{b_1} - 1\right)(1-h_c)\right] \tag{9}$$

For the geometry of Fig. 1b,

$$\frac{Ch_c'^{1/n}}{\sigma_{H_c'}} = \beta^{1/n}h_t'^{2+1/n}\left[\frac{b_2}{b_1} - \left(\frac{n}{3n+1}\right)\left(\frac{b_2}{b_1}\right) - 1\ h_t'\right] + (1-h_t')^{2+1/n}\left[1 + \left(\frac{n}{3n+1}\right)\left(\frac{b_2}{b_1} - 1\right)(1-h_t')\right]. \tag{10}$$

These equations can be used to calculate the outer fibre stress for a given cross-section and moment, provided β is known. Rearrangement of these equations allows β to be determined.

The outer fibre surface strain is related to the radius of curvature by $\epsilon_{h_c} = -H_c/R$. By rearranging and using Equation 1 the radius of curvature for geometry (a) is given by;

$$1/R = \beta\sigma_{H_c}^n F(t)/H_c, \tag{11}$$

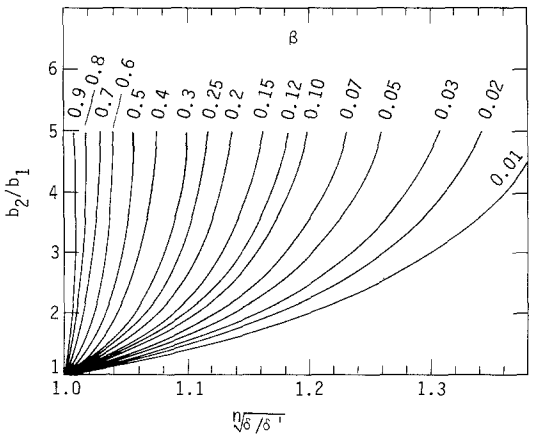

Figure 3 Graphical solutions of Equation 13 for $n = 2$. This graph is used to determine β from measured values of $\sqrt[n]{\delta/\delta'}$ and b_2/b_1.

and similarly for geometry (b);

$$1/R' = \beta\sigma_{H_c}'^{n} F(t)/H_c'. \tag{12}$$

Equation 3 is used to relate beam deflection to the radius of curvature; thus

$$\sqrt[n]{\frac{\delta}{\delta'}} = \sqrt[n]{\frac{1/R}{1/R'}} = \frac{\text{Right hand side Equation 10}}{\text{Right hand side Equation 9}}. \tag{13}$$

Fig. 3 is a graph of the relationship between $\sqrt[n]{\delta/\delta'}$ and b_2/b_1 for several values of β and $n = 2$. Observation of δ and δ' at several times, for which creep strains are large compared to the initial elastic strains at constant moment allows us to determine the ratio of compressive creep to tensile creep (see Fig. 3). Once β is known the distance from the neutral axis (h_c) can be determined from Fig. 2. If the stress exponent, n, is unknown one can determine it by the usual graphical method as illustrated in Section 4.3 of this paper, or Equations 7, 9 and 10 can be programmed in a computer and the values of h_c, β, and n determined numerically from measurements of δ/δ'.

If δ/δ' varies greatly with time this analysis is not applicable. If $\beta = 1$, tension and compressive creep are the same and the usual bend equations are valid. If $\beta \neq 1$, then the individual creep rates for tensile and compressive creep can be determined. Once β and h_c are known, Equation 9 is used to calculate σ_{H_c}. For this purpose, Fig. 4, a graph of $Ch_c^{1/n}/\sigma_{H_c}$ for various b_2/b_1 ratios and β's, is provided. Measurement of curvature as a function of time allows determination of $F(t)$ from Equation 11. Equation 1A can then be used to determine the individual compressive and tensile creep rates. The following section illustrates how these relationships are used to determine the compressive and tensile creep behaviour of HS-130 Si_3N_4.

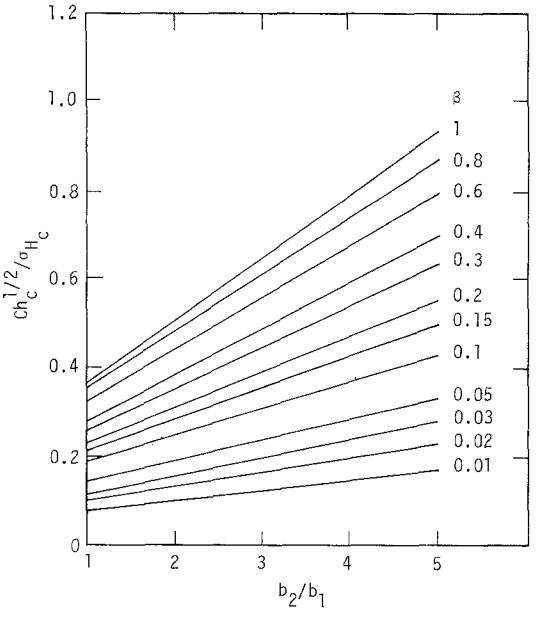

Figure 4 Graph of quantity used to obtain σ_{H_c} (outer fibre compressive stress) as a function of b_2/b_1 for several values of β. See Equation 9 in text.

3. Experimental

Four-point bending tests were conducted on Si_3N_4 beams in a tubular furnace open to the atmosphere. Deflection of the beam between the inner load points was measured directly using a differential probe technique. The deflection probe rods were capped with Si_3N_4 to prevent reactions on the surface of the test bar. The deflection was recorded continuously with a displacement transducer and a strip chart recorder.

Deflection rates as low as 1.2×10^{-6} m h^{-1} could be measured. The load was applied by hanging weights from the top fixture of the load train. The temperature was controlled to within $\pm 2°$ C during each test.

All the test bars were machined from the same HS-130 Si_3N_4 billet. Beam geometries with b_2/b_1 ratios of 3.24 and 2.40 were used in the tests. The b_1 dimension was 0.72 cm and the height, H, was 0.318 cm in both cases. The inner span of the test fixture was 1.91 cm long.

TABLE I Test conditions for tests of HS-130 Si_3N_4.

Test No.	Temperature (° C)	b_2/b_1	Moment (N m)	$\dot{\delta}$ (10^{-6} m h^{-1})	$\sqrt[n]{\delta/\delta'}$	β	h_c	σ_{H_c} MN m^{-2}	σ_{H_t} (MN m^{-2})	$\dot{\epsilon}_{H_c}$ (10^{-4} h^{-1})	$\dot{\epsilon}_{H_t}$ (10^{-4} h^{-1})
1	1300	3.24	0.752	4.242	1.10	0.24	0.29	85.6	65.6	0.86	2.10
2	1293	3.24	1.947	22.098	1.14	0.14	0.26	247.2	156.04	4.01	11.40
3*	1298	3.24	1.344	9.652	1.05	0.48	0.34	130.7	126.16	2.29	4.44
4	1260	2.40	1.105	3.253	1.10	0.17	0.28	163.5	108.10	0.64	1.63
5	1253	2.40	1.482	5.105	1.10	0.17	0.28	219.3	145.0	1.00	2.56

*Presented (retest of bars from test No. 1).

4. Results and discussion

4.1. Determination of β and h_c

The determination of β and h_c requires that identical bend bars be tested under the same moment and temperature conditions in the orientations shown in Fig. 1. The following procedure is based upon knowledge that the stress exponent, n, for Si_3N_4 is approximately 2. This value can also be determined directly from the data using the usual technique of plotting log creep rate versus log stress (see Section 4.3). The centre point deflections δ and δ' are then recorded as functions of time. Fig. 5 shows deflection curves for two Si_3N_4 bars tested at 1300° C and 0.745 N m bending moment, along with the ratio δ/δ' at several times. The ratio of compressive to tensile creep strain, β, is then determined from Fig. 3 for the b_2/b_1 geometry used and for the experimentally determined $\sqrt[n]{\delta/\delta'}$. Fig. 2 is then used to determine h_c and h_t' using β and β^{-1} respectively. Table I summarizes test conditions and results for five sets of tests conducted on HS-130 Si_3N_4. Tabulated values for β and h_c are based on the steady-state deflection ratio $\sqrt[n]{\delta/\delta'}$ at each of the temperatures tested. If δ/δ' is found to vary greatly with time, this analysis is not applicable.

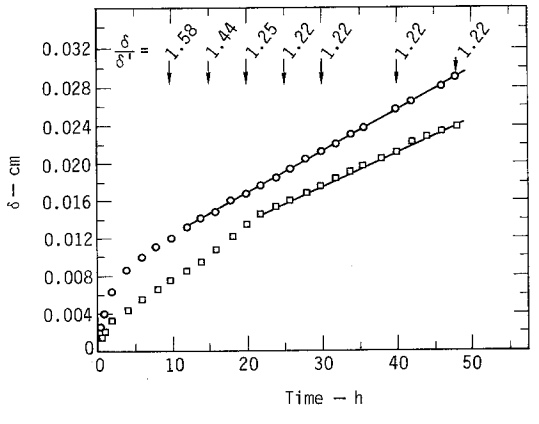

Figure 5 Creep curves obtained from two trapezoidal HS-HS-130 Si_3N_4 bars tested at 1300° C and 0.752 Nm. δ and δ' are the centre-point deflections measured on bars oriented as shown in Figs. 1a and 1b respectively. The ratio of the centre-point deflections δ/δ' is presented at several different times. The steady-state deflection rate ($\dot{\delta}$) is given for geometry 1a. ($\dot{\delta} = 4.2 \times 10^{-4}$ cm h^{-1}).

4.2. Determination of stresses and creep rates

Once β and h_c are known, the individual tensile and compressive stresses and creep rates can be calculated. The outer fibre compressive stress, σ_{h_c}, and the corresponding tensile stress, σ_{h_t}, are calculated by using Fig. 4 and Equation 5, respectively. Using $1/R = \dfrac{8\delta}{l^2}$ and substituting into Equation 11 allows us to calculate $F(t)$ from the measurement of curvature as a function of time. The constant creep rates $\dot{\epsilon}_{H_c}$ and $\dot{\epsilon}_{H_t}$ are obtained by inserting the observed deflection rate, $\dot{\delta}$, and stress at the outer fibre into the time derivatives of Equation 1 and Equation 11 with $A = 1$ for tension and $A = \beta$ for compression.

4.3. Determination of the stress exponent, n

The dependence of creep rate on n is required in order to perform correctly the analysis described above. One way to determine n from trapezoidal bend-bar tests is to perform tests at different loads and identical temperatures initially assuming $n = 1$. The assumption that $\beta = 1$ (i.e., the neutral axis lies in the centroidal plane) may also be made and has little effect on the resulting approximation of n. The analysis allows a plot of log strain rate versus log stress to be made, from which the value for n may be determined as the slope of the line. Data points denoted by squares in Fig. 6 represent the analysis of tests 1 and 2, assuming n and β are equal to one. It may be seen from Fig. 6 that a better approximation would be $n = 2$. Data denoted by circles represent the analysis based upon $n = 2$.

For compression with our 1300° C results, data from Lenoe [4], obtained in air on HS-130 Si_3N_4 from uniaxial tensile tests (and corrected to 1300° C

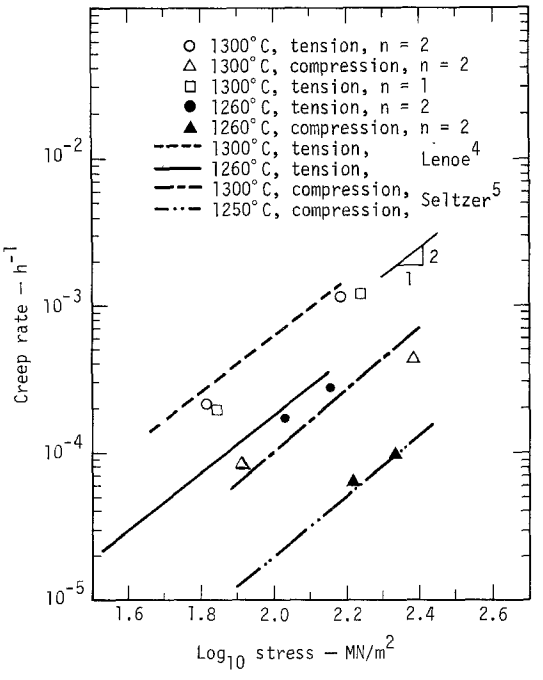

Figure 6 Graph of creep rate versus log stress comparing our results with creep rate data obtained from the literature. The upper two lines shows the creep rate of HS-130 Si_3N_4 as measured in direct tension tests and the lower two lines show creep rate measured in compression tests.

by the authors assuming an activation energy of $Q = 0.63\,MJ\,mol^{-1}$ [4], are represented by a dashed line in Fig. 5.

Our compressive creep rates are shown in Fig. 6 and were determined in a similar fashion. For comparision, compressive creep data obtained in air on HS-130 Si_3N_4 by Seltzer [5] are also given in Fig. 6. The agreement is good for both the tensile and compressive creep rates calculated from the trapezoidal bend bar tests. Results of tests performed at 1260° C also agree with Leone's and Seltzer's work.

Test number 3 (Table I) was performed on a previously tested bar and shows a smaller difference between the tensile and compressive creep rates. Also, the tensile creep rate is lower than the results obtained from unstrained material. This difference between strained and unstrained material has also been observed by Sletzer [5].

4.4. Reanalysis of published creep data

Osborne [10] also performed four-point bend tests on Norton Co. HS-130 Si_3N_4. He reported a steady-state creep rate of $1.1 \times 10^{-5}\,h^{-1}$ (1227° C and an outer fibre stress of $77\,MN\,m^{-2}$). His value falls between the true tensile and compressive rates as reported in the literature [4–6]*. Using the analysis technique developed in this paper, it is possible to reanalyse Osborne's data and determine individual tensile and compressive creep rates.

TABLE II Osborne's published creep data [10].

b_2/b_1	$M(\sigma = My/I)$ (N m)	$H(=b_1)$ (mm)	L (mm)	$\dot{\epsilon}_{ss}$ (at 1260° C) (h^{-1})
1	0.42	3.2	25.4	2.75×10^{-5}

We have shown that the ratio of compressive creep to tensile creep in HS-130 Si_3N_4 is $\beta = 0.18$ (average of four tests on previously unstrained material). From Osborne's data (see Table II), we known that $b_2/b_1 = 1$. Fig. 4 can then be used to determine σ_{H_c} ($83.6\,MN\,m^{-2}$), and Equation 11 used to get $F(t)$ as a function of the measured creep strain $[\epsilon_{meas} = (H/2R)]$. Substituting $F(t)$ into Equation 1 and taking the derivative gives the expression for tensile creep;

$$\dot{\epsilon}_t = 2(\sigma_t/\sigma_{H_c})^n \dot{\epsilon}_{ss}(h_c)(1/\beta).$$

For compressive creep the $(1/\beta)$ term is removed. When Osborne's data are used in these expressions we get

$$\dot{\epsilon}_t = 1.10 \times 10^{-4}\,h^{-1} \text{ at } 83.6\,MN\,m^{-2} \text{ and } 1260°\,C$$

and

$$\dot{\epsilon}_c = 1.98 \times 10^{-5}\,h^{-1} \text{ at } 83.6\,MN\,m^{-2} \text{ and } 1260°\,C.$$

The values we get from Fig. 5 under the same conditions are

$$\dot{\epsilon}_t = 1.2 \times 10^{-4}\,h^{-1}$$

and

$$\dot{\epsilon}_c = 1.4 \times 10^{-5}\,h^{-1}.$$

This is excellent agreement.

6. Conclusions

The following conclusions may be drawn from the present investigation:

(1) The tensile and compressive creep behaviour of a material can be determined from four-point bending tests on beams having trapezoidal cross-sections.

(2) The analysis can be used to determine the stress exponent n, the ratio of compressive to ten-

*This steady-state creep rate increases by a factor of $\simeq 2.5$ with a 30° C temperature increase. $\dot{\epsilon}_{ss} \simeq 2.75 \times 10^{-5}\,h^{-1}$ at 1260° C.

sile creep strain, β, and the outer fibre tensile and compressive stresses.

(3) The addition of the parameter β complicates the analysis of test data, but allows a more accurate determination of material response.

(4) The parameter β drastically alters the relationship observed between creep strain rates and stresses, in the case of Si_3N_4, by at least half an order of magnitude.

(5) Individual tensile and compressive creep rates can be determined from conventional four-point bend tests once the parameter β is known.

References

1. R. K. PENNY, E. G. ELLISION and G. H. WEBSTER, *Mater. Res and Stds* **6** (1966) 76.
2. G. W. HOLLENBERG, G. R. TERWILLIGER and R. S. GORDON, *J. Amer. Ceram. Soc.* **56** (1971) 196.
3. I. FINNIE and W. R. HELLER, "Creep of Engineering Materials" (1959) p. 135.
4. E. M. LENOE and G. D. QUINN, "Deformation of Ceramic Materials", edited by R. C. Bradt and R. E. Tressler (1975) p. 399.
5. M. S. SELTZER, High Temperature Creep of Ceramics, Final Report, AFML-TR-76-97 (1976).
6. A. F. MCLEAN, E. A. FISHER and J. R. BRATTON, Brittle Materials Design, High Temperature Gas Turbine, AMMRC CTR 74-26 (1974).
7. F. F. LANGE, "Deformation of Ceramic Materials", edited by R. C. Bradt and R. E. Tressler, (1975) p. 361.
8. I. FINNIE, *J. Amer. Ceram. Soc.* **49** (1966) 218.
9. G. R. TREWILLIGER and K. C. RADFORD, *Amer. Ceram. Soc. Bull.* **53** (1974) 173.
10. N. J. OSBORNE, *Proc. Brit. Ceram. Soc.* **26** (1975) 263.

Received 28 July 1976 and accepted 5 July 1977.